ISSN 2347-3487

EXCITON INSULATOR STATES IN MATERIALS WITH 'MEXICAN HAT' BAND STRUCTURE DISPERSION AND IN GRAPHENE.

Lyubov E. Lokot
Institute of Semiconductor Physics, NAS of Ukraine, 41, Nauky Ave., Kyiv 03028, Ukraine
llokot@gmail.com

Abstract

In the paper a theoretical study the both the quantized energies of excitonic states and their wave functions in graphene and in materials with "Mexican hat" band structure dispersion as well as in zinc-blende GaN is presented. An integral two-dimensional Schrödinger equation of the electron-hole pairing for a particles with electron-hole symmetry of reflection is exactly solved. The solutions of Schrödinger equation in momentum space in studied materials by projection the two-dimensional space of momentum on the three-dimensional sphere are found exactly. We analytically solve an integral two-dimensional Schrödinger equation of the electron-hole pairing for particles with electron-hole symmetry of reflection. In studied materials the electron-hole pairing leads to the exciton insulator states. Quantized spectral series and light absorption rates of the excitonic states which distribute in valence cone are found exactly. If the electron and hole are separated, their energy is higher than if they are paired. The particle-hole symmetry of Dirac equation of layered materials allows perfect pairing between electron Fermi sphere and hole Fermi sphere in the valence cone and conduction cone and hence driving the Cooper instability. The solutions of Coulomb problem of electron-hole pair does not depend from a width of band gap of graphene. It means the absolute compliance with the cyclic geometry of diagrams at justification of the equation of motion for a microscopic dipole of graphene where $r_s > 1$. The absorption spectrums for the zinc-blende GaN/(Al,Ga)N quantum well as well as for the zinc-blende bulk GaN are presented. Comparison with available experimental data shows good agreement.

Indexing terms/Keywords

Particle-hole pair; 'Mexican hat'; quantum well; grapheme; Dirac cone.

Council for Innovative Research
Peer Review Research Publishing System
Journal: JOURNAL OF ADVANCES IN PHYSICS
Vol. 11, No. 1
www.cirjap.com, japeditor@gmail.com

1 Introduction

The graphene [1-5] presents a new state of matter of layered materials. The energy bands for graphite was found using "tight-binding" approximation by P.R. Wallace [6]. In the low-energy limit the single-particle spectrum is Dirac cone similarly to the light cone in relativistic physics, where the light velocity is substituted by the Fermi velocity $v_F = 10^6$ m/s and is described by the massless Dirac equation.

In the paper we present a theoretical investigation of excitonic states as well as their wave functions in graphene and in materials with "Mexican hat" band structure dispersion as well as in zinc-blende GaN. An integral form of the two-dimensional Schrödinger equation of Kepler problem in momentum space is solved exactly by projection the two-dimensional space of momentum on the three-dimensional sphere in the paper [7].

The integral Schrödinger equation was analytically solved by the projection the three-dimensional momentum space onto the surface of a four-dimensional unit sphere by Fock in 1935 [8].

We consider the pairing between oppositely charged particles with complex dispersion. The Coulomb interaction leads to the electron-hole bound states scrutiny study of which acquire significant attention in the explanations of superconductivity.

If the exciton binding energy is greater than the flat band gap in narrow-gap semiconductor or semimetal then at sufficiently low temperature the insulator ground state is instable with respect to the exciton formation [9-12]. And excitons may be spontaneously created. In a system undergo a phase transition into a exciton insulator phase similarly to Bardeen-Cooper-Schrieffer (BCS) superconductor. In a single-layer graphene (SLG) the electron-hole pairing leads to the exciton insulator states [13].

In the paper an integral two-dimensional Schrödinger equation of the electron-hole pairing for particles with complex dispersion is analytically solved. A complex dispersions lead to fundamental difference in exciton insulator states and their wave functions.

We analytically solve an integral two-dimensional Schrödinger equation of the electron-hole pairing for particles with electron-hole symmetry of reflection.

For graphene in vacuum the effective fine structure parameter $r_s = \dfrac{e^2}{v_F \hbar \kappa \sqrt{\pi}} = 1.23$. For graphene in substrate $r_s = 0.77$, when the permittivity of graphene in substrate is estimated to be $\kappa = 1.6$ [14]. It means the prominent Coulomb effects [15].

It is known that the Coulomb interaction leads to the semimetal-exciton insulator transition, where gap is opened by electron-electron exchange interaction [9,16-18]. The perfect host combines a small gap and a large exciton binding energy [9,12].

In graphene the existing of bound pair states are still subject matter of researches [19-23].

It is known [24] in the weak-coupling limit [25], exciton condensation is a consequence of the Cooper instability of materials with electron-hole symmetry of reflection inside identical Fermi surface. The identical Fermi surfaces is a consequence of the particle-hole symmetry of massless Dirac equation for Majorana fermions.

A deeper understanding of the influence of band structures on optical properties should help one to answer many questions. In addition, the interesting effects of strong electron-hole Coulomb interaction are presented in these materials. Many-body interactions lead to effects, which consist the screening, dephasing, bandgap renormalization, and phase-space filling [26-29].

A general phenomenon of Coulomb enhancement may be explained as follows. Due to the Coulomb attraction, an electron and a hole have a larger tendency to be located near each other, than that in the case of noninteracting particles. This increase of the interaction duration leads to an increase of the optical transition probability.

2 Equation of motion for a microscopic dipole.

The Heisenberg equation for a microscopic dipole, $\hat{p}_{\mathbf{p}}^{\nu_e \nu_h} = \langle \hat{b}_{-\mathbf{p}} \hat{a}_{\mathbf{p}} \rangle$ is written in the form:

$$\frac{\partial \hat{p}_{\mathbf{p}}^{\nu_e \nu_h}}{\partial t} = \frac{i}{\hbar} [\hat{H}, \hat{p}_{\mathbf{p}}^{\nu_e \nu_h}]. \tag{1}$$

To make the analysis as simple as possible, we assume a nondegenerate situation described by the Hamiltonian $\hat{H} = \hat{H}_0 + \hat{V} + \hat{H}_{int}$, which is composed of the kinetic energy of an electron $\varepsilon_{e,\mathbf{p}}^{\nu_e}$ and the kinetic energy of a hole $\varepsilon_{h,\mathbf{p}}^{\nu_h}$ in the electron-hole representation:

$$\hat{H}_0 = \sum_{\mathbf{p}} \varepsilon_{e,\mathbf{p}}^{\nu_e} \hat{a}_{\mathbf{p}}^{+} \hat{a}_{\mathbf{p}} + \varepsilon_{h,\mathbf{p}}^{\nu_h} \hat{b}_{-\mathbf{p}}^{+} \hat{b}_{-\mathbf{p}}, \tag{2}$$

where **p** is the transversal quasimomentum of carriers in the plane of the quantum well, $\hat{a}_{\mathbf{p}}$, $\hat{a}_{\mathbf{p}}^{+}$, $\hat{b}_{-\mathbf{p}}$, and $\hat{b}_{-\mathbf{p}}^{+}$ are the annihilation and creation operators of an electron and a hole. The Coulomb interaction Hamiltonian for particles in the electron-hole representation takes the form:

$$\hat{V} = \frac{1}{2} \sum_{\mathbf{p},\mathbf{k},\mathbf{q}} V_q^{\nu_e \nu_e \nu_e \nu_e} \hat{a}_{\mathbf{p}+\mathbf{q}}^{+} \hat{a}_{\mathbf{k}-\mathbf{q}}^{+} \hat{a}_{\mathbf{k}} \hat{a}_{\mathbf{p}} +$$

$$+ V_q^{\nu_h \nu_h \nu_h \nu_h} \hat{b}_{\mathbf{p}+\mathbf{q}}^{+} \hat{b}_{\mathbf{k}-\mathbf{q}}^{+} \hat{b}_{\mathbf{k}} \hat{b}_{\mathbf{p}} -$$

$$- 2V_q^{\nu_e \nu_h \nu_h \nu_e} \hat{a}_{\mathbf{p}+\mathbf{q}}^{+} \hat{b}_{\mathbf{k}-\mathbf{q}}^{+} \hat{b}_{\mathbf{k}} \hat{a}_{\mathbf{p}}, \tag{3}$$

where

$$V_q^{\nu_\alpha \nu_\beta \nu_\beta \nu_\alpha} = \frac{e^2}{\varepsilon} \frac{1}{A} \int_{-w/2}^{+w/2} dz \int_{-w/2}^{+w/2} dz' \chi_{\nu_\alpha}(z) \chi_{\nu_\beta}(z') \frac{2\pi}{q} \times$$

$$\times e^{-q|z-z'|} \chi_{\nu_\beta}(z') \chi_{\nu_\alpha}(z), \tag{4}$$

is the Coulomb potential of the quantum well, ε is the dielectric permittivity of a host material of the quantum well, and A is the area of the quantum well in the xy plane.

The Hamiltonian of the interaction of a dipole with an electromagnetic field is described as follows:

$$\hat{H}_{\text{int}} = -\frac{1}{A} \sum_{\nu_e, \nu_h, \mathbf{p}} ((\mu_{\mathbf{p}}^{\nu_e \nu_h})^{*} \hat{p}_{\mathbf{p}}^{\nu_e \nu_h} E^{*} e^{i\omega t} +$$

$$+ (\mu_{\mathbf{p}}^{\nu_e \nu_h})(\hat{p}_{\mathbf{p}}^{\nu_e \nu_h})^{+} E e^{-i\omega t}), \tag{5}$$

where $\hat{p}_{\mathbf{p}}^{\nu_e \nu_h} = \langle \hat{b}_{-\mathbf{p}} \hat{a}_{\mathbf{p}} \rangle$ is a microscopic dipole due to an electron-hole pair with the electron (hole) momentum **p** (–**p**) and the subband number ν_e (ν_h), $\mu_{\mathbf{k}}^{\nu_e \nu_h} = \int d^3 r U_{j'\sigma'\mathbf{k}} \mathbf{e} \hat{\mathbf{p}} U_{j\sigma\mathbf{k}}$, is the matrix element of the electric dipole moment, which depends on the wave vector **k** and the numbers of subbands, between which the direct interband transitions occur, $\mathbf{e}$ is a unit vector of the vector potential of an electromagnetic wave, $\hat{\mathbf{p}}$ is the momentum operator. Subbands are described by the wave functions $U_{j'\sigma'\mathbf{k}}$, $U_{j\sigma\mathbf{k}}$, where j' is the number of a subband from the conduction band, σ' is the electron spin, j is the number of a subband from the valence band, and σ is the hole spin. We consider one lowest conduction subband $j'=1$ and one highest valence subband $j=1$. E and ω are the electric field amplitude and frequency of an optical wave.

Estimating the ratio of the Coulomb potential energy to the Fermi energy for GaN, we obtain

$$r_s = \frac{E_{\text{C}}}{E_{\text{F}}} = \frac{2me^2}{\varepsilon \hbar^2 \sqrt{n\pi}} = 0.73 \tag{6}$$

for the concentration of the electron-hole gas $n = 10^{13}$ cm^{-2}, the dielectric permittivity $\varepsilon = 9.38$, the transversal effective mass of an electron at Γ point $m = 0.18$ (inverse second derivative of the energy with respect to the transversal wave vector). This indicates that the Fermi energy dominates relative to the Coulomb potential energy as $r_s \to 0$ and increases more rapidly than the Coulomb energy with the increasing density. As $r_s \to 0$ the terms corresponding to cyclic diagrams will dominate.

Thus we consider the approximation which simplifies the calculations in solving the problem concerning the electron-hole gas on the one hand. Because we solved the problem in the case of a high density of the electron-hole gas (case $r_s < 1$).

However as one can see the solutions of Coulomb problem of electron-hole pair does not depend from a width of band gap of graphene. Hence accepted approximation may be proved for the case $r_s > 1$. It means the absolute compliance with the cyclic geometry of diagrams at justification of the equation of motion for a microscopic dipole of graphene where $r_s > 1$ (see such as [18]).

In this section, we derive the equation of motion for the mean value of the product $\hat{b}_{-\mathbf{p}}\hat{a}_{\mathbf{p}}$ for a microscopic dipole, which specifies of a medium polarization, which becomes macroscopic due to the applied external field.

The average value of a certain physical magnitude F, which corresponds to the operator $\hat{F}$ can be expressed through the spur of a matrix, which is a certain statistic operator obeying the Heisenberg equation:

$$\langle \hat{F} \rangle = \mathrm{S}p(\hat{w}_0 \hat{F}) +$$

$$+\frac{2\pi}{i} D(-\varepsilon_{\mathbf{p}_1+\mathbf{q}} - \varepsilon_{\mathbf{p}_2-\mathbf{q}} + \varepsilon_{\mathbf{p}_1} + \varepsilon_{\mathbf{p}_2})\mathrm{S}p([\hat{F}, \hat{V}_0]\hat{w}_0), \tag{7}$$

where $\hat{w}_0 = \dfrac{e^{-\hat{H}_0/kT}}{\mathrm{S}p(e^{-\hat{H}_0/kT})}$, i.e., the density matrix $\hat{w}_0$ is assumed to be described by the Gibbs canonical distribution; in the interaction representation, the time dependences of a wave function and any certain operator can be expressed through the Hamiltonian of a system of noninteracting particles: $\hat{V}_0 = = e^{i\hat{H}_0 t/\hbar} \hat{V} e^{-i\hat{H}_0 t/\hbar}$.

One can find the expectation value from the convolution of two operators: $\langle \hat{a}^+_{\mathbf{k}} \hat{a}_{\mathbf{p}}(\tau) \rangle$ regarding the density matrix, i.e. the certain statistic operator $\rho = \dfrac{e^{-\beta H_0}}{Sp(e^{-\beta H_0})}$. From the Heisenberg equation, we obtain

$$\langle \hat{a}_{\mathbf{p}} \hat{a}^+_{\mathbf{k}} \rangle = e^{\beta \varepsilon^{\nu_e}_{\mathbf{p}}} \langle \hat{a}^+_{\mathbf{k}} \hat{a}_{\mathbf{p}} \rangle. \tag{8}$$

Since $\hat{a}_{\mathbf{p}} \hat{a}^+_{\mathbf{k}} = \delta_{\mathbf{pk}} - \hat{a}^+_{\mathbf{k}} \hat{a}_{\mathbf{p}}$ for fermions (8) yields the expression for the electron population in terms of the Fermi distribution function:

$$\langle \hat{a}^+_{\mathbf{k}} \hat{a}_{\mathbf{p}} \rangle = \frac{\delta_{\mathbf{pk}}}{1 + e^{\beta \varepsilon^{\nu_e}_{\mathbf{p}}}}, \tag{9}$$

where $\varepsilon^{\nu_e}_{\mathbf{p}} = \varepsilon^{\nu_e}_{\mathbf{p}} - E_{\mathrm{F}}$, and E_{F} is the Fermi energy.

The Heisenberg equation for the electron-hole gas takes the form

$$\frac{d\hat{p}^{\nu_e\nu_h}_{\mathbf{p}}}{dt} = -i\omega^{\nu_e\nu_h}_{\mathbf{p}} \hat{p}^{\nu_e\nu_h}_{\mathbf{p}} - i\Omega^{\nu_e\nu_h}_{\mathbf{p}} (-1 + \hat{n}^{\nu_e}_{\mathbf{p}} + \hat{n}^{\nu_h}_{\mathbf{p}}) +$$

$$+\frac{i}{\hbar}(\sum_{\mathbf{q},\mathbf{k}} V^{\nu_e\nu_e\nu_e\nu_e}_q \langle \hat{a}^+_{\mathbf{k}+\mathbf{q}} \hat{a}_{\mathbf{p}+\mathbf{q}} \hat{b}_{-\mathbf{p}} \hat{a}_{\mathbf{k}} \rangle +$$

$$+V^{\nu_h\nu_h\nu_h\nu_h}_q \langle \hat{b}^+_{\mathbf{k}+\mathbf{q}} \hat{b}_{-\mathbf{p}+\mathbf{q}} \hat{b}_{\mathbf{k}} \hat{a}_{\mathbf{p}} \rangle -$$

$$-\sum_{\mathbf{q},\mathbf{k}} V^{\nu_e\nu_h\nu_h\nu_e}_q ((\langle \hat{a}^+_{\mathbf{k}+\mathbf{q}} \hat{a}_{\mathbf{p}} \hat{b}_{-\mathbf{p}+\mathbf{q}} \hat{a}_{\mathbf{k}} \rangle +$$

$$+\langle \hat{b}^+_{\mathbf{k}+\mathbf{q}} \hat{b}_{-\mathbf{p}} \hat{b}_{\mathbf{k}} \hat{a}_{\mathbf{p}+\mathbf{q}} \rangle - \langle \hat{b}_{-\mathbf{p}+\mathbf{q}} \hat{a}_{\mathbf{p}-\mathbf{q}} \rangle \delta_{\mathbf{q},\mathbf{k}})), \tag{10}$$

where $\omega_{\mathbf{p}}^{\nu_e\nu_h}=\frac{1}{\hbar}(\varepsilon_{g0}+\varepsilon_{e,\mathbf{p}}^{\nu_e}+\varepsilon_{h,\mathbf{p}}^{\nu_h})$, $\Omega_{\mathbf{p}}^{\nu_e\nu_h}=\frac{1}{\hbar}\mu_{\mathbf{p}}^{\nu_e\nu_h}Ee^{-i\omega t}$. The electron and hole populations are as follows $\hat{n}_{\mathbf{p}}^{\nu_e}=\langle\hat{a}_{\mathbf{p}}^{+}\hat{a}_{\mathbf{p}}\rangle$, $\hat{n}_{\mathbf{p}}^{\nu_h}=\langle\hat{b}_{-\mathbf{p}}^{+}\hat{b}_{-\mathbf{p}}\rangle$.

Using the operator algebra and the density matrix formalism as well as diagram method based on cyclic geometry of diagrams, we have

$$
\begin{gathered}
\frac{d\hat{p}_{\mathbf{p}}^{\nu_e\nu_h}}{dt}=-i\omega_{\mathbf{p}}^{\nu_e\nu_h}\hat{p}_{\mathbf{p}}^{\nu_e\nu_h}-i\Omega_{\mathbf{p}}^{\nu_e\nu_h}(-1+\hat{n}_{\mathbf{p}}^{\nu_e}+\hat{n}_{\mathbf{p}}^{\nu_h})- \\
-\frac{i}{\hbar}\sum_{\mathbf{q}}V_q^{\nu_e\nu_h\nu_h\nu_e}\hat{p}_{\mathbf{p+q}}^{\nu_e\nu_h}(-1+\hat{n}_{\mathbf{p}}^{\nu_e}+\hat{n}_{\mathbf{p}}^{\nu_h})- \\
-\frac{i}{\hbar}\sum_{\mathbf{q}}W_q^{\nu_e\nu_h\nu_h\nu_e}\hat{p}_{\mathbf{p+q}}^{\nu_e\nu_h}(\Xi_{\mathbf{p,q}}^{\nu_e}+\Xi_{\mathbf{p,q}}^{\nu_h})+ \\
+\frac{1}{\hbar}\sum_{\substack{\alpha=e,h\\ \beta=e,h\\ \alpha\neq\beta}}\sum_{\nu_\alpha,\nu_\beta}\sum_{\mathbf{k,q}}W_q^{\nu_\alpha\nu_\beta\nu_\beta\nu_\alpha}W_{|p+q-k|}^{\nu_\alpha\nu_\beta\nu_\beta\nu_\alpha}\times \\
\times D(\varepsilon_{\mathbf{p}}^{\nu_\beta}+\varepsilon_{\mathbf{k}}^{\nu_\alpha}-\varepsilon_{\mathbf{k-q}}^{\nu_\beta}-\varepsilon_{\mathbf{p+q}}^{\nu_\alpha})\times \\
\times(\hat{n}_{\mathbf{p}}^{\nu_\beta}(1-\hat{n}_{\mathbf{k-q}}^{\nu_\beta})\hat{n}_{\mathbf{k}}^{\nu_\alpha}+(1-\hat{n}_{\mathbf{p}}^{\nu_\beta})\hat{n}_{\mathbf{k-q}}^{\nu_\beta}(1-\hat{n}_{\mathbf{k}}^{\nu_\alpha}))\hat{p}_{\mathbf{p+q}}^{\nu_e\nu_h}. \qquad (11)
\end{gathered}
$$

Equation (11) describes the oscillation of the polarization at the transition frequency and the processes of stimulated emission or absorption. As the population functions, we choose the Fermi distribution functions. The transition frequency $\omega_{\mathbf{p}}^{\nu_e\nu_h}$ is derived as follows:

$$
\begin{gathered}
\omega_{\mathbf{p}}^{\nu_e\nu_h}=\frac{1}{\hbar}(\varepsilon_{g0}+\varepsilon_{e,\mathbf{p}}^{\nu_e}+\varepsilon_{h,\mathbf{p}}^{\nu_h}+ \\
+\sum_{\alpha=e,h}\sum_{\nu_\alpha}\sum_{\mathbf{q}}(V_q^{\nu_\alpha\nu_\alpha\nu_\alpha\nu_\alpha}(-\hat{n}_{\mathbf{p+q}}^{\nu_\alpha})+ \\
+W_q^{\nu_\alpha\nu_\alpha\nu_\alpha\nu_\alpha}(-\hat{\Xi}_{\mathbf{p+q,q}}^{\nu_\alpha}))- \\
-i\sum_{\substack{\alpha=e,h\\ \beta=e,h\\ \alpha\neq\beta}}\sum_{\nu_\alpha,\nu_\beta}\sum_{\mathbf{k,q}}(W_q^{\nu_\alpha\nu_\beta\nu_\beta\nu_\alpha})^2\times \\
\times D(-\varepsilon_{\mathbf{p+q}}^{\nu_\alpha}-\varepsilon_{\mathbf{k-q}}^{\nu_\beta}+\varepsilon_{\mathbf{k}}^{\nu_\beta}+\varepsilon_{\mathbf{p}}^{\nu_\alpha})\times \\
\times(\hat{n}_{\mathbf{k-q}}^{\nu_\beta}(1-\hat{n}_{\mathbf{k}}^{\nu_\beta})\hat{n}_{\mathbf{p+q}}^{\nu_\alpha}+(1-\hat{n}_{\mathbf{k-q}}^{\nu_\beta})\hat{n}_{\mathbf{k}}^{\nu_\beta}(1-\hat{n}_{\mathbf{p+q}}^{\nu_\alpha})). \qquad (12)
\end{gathered}
$$

The functions $\hat{\Xi}_{\mathbf{p+q,q}}^{\nu_e}$ and $\hat{\Xi}_{\mathbf{p,q}}^{\nu_e}$ are defined as

$$
\begin{gathered}
\hat{\Xi}_{\mathbf{p+q,q}}^{\nu_e}=i\sum_{\mathbf{k}}[W_q^{\nu_e\nu_e\nu_e\nu_e}-W_{|k-q-p|}^{\nu_e\nu_e\nu_e\nu_e}]\times \\
\times D(-\varepsilon_{\mathbf{p+q}}^{\nu_e}-\varepsilon_{\mathbf{k-q}}^{\nu_e}+\varepsilon_{\mathbf{k}}^{\nu_e}+\varepsilon_{\mathbf{p}}^{\nu_e})\times
\end{gathered}
$$

$$\times(\hat{n}^{\nu_e}_{\mathbf{k-q}}(1-\hat{n}^{\nu_e}_{\mathbf{k}})\hat{n}^{\nu_e}_{\mathbf{p+q}}+(1-\hat{n}^{\nu_e}_{\mathbf{k-q}})\hat{n}^{\nu_e}_{\mathbf{k}}(1-\hat{n}^{\nu_e}_{\mathbf{p+q}})), \tag{13}$$

$$\hat{\Xi}^{\nu_e}_{\mathbf{p,q}}=i\sum_{\mathbf{k}}[W_q^{\nu_e\nu_e\nu_e\nu_e}-W_{|k+q-p|}^{\nu_e\nu_e\nu_e\nu_e}]\times$$

$$\times D(-\varepsilon^{\nu_e}_{\mathbf{p+q}}-\varepsilon^{\nu_e}_{\mathbf{k-q}}+\varepsilon^{\nu_e}_{\mathbf{k}}+\varepsilon^{\nu_e}_{\mathbf{p}})\times$$

$$\times((1-\hat{n}^{\nu_e}_{\mathbf{k}})\hat{n}^{\nu_e}_{\mathbf{k-q}}(1-\hat{n}^{\nu_e}_{\mathbf{p}})+\hat{n}^{\nu_e}_{\mathbf{k}}(1-\hat{n}^{\nu_e}_{\mathbf{k-q}})\hat{n}^{\nu_e}_{\mathbf{p}}). \tag{14}$$

We have replaced the bare Coulomb potential energy with the screened one:

$$V_q(1-VM+(VM)^2-(VM)^3+\ldots), \tag{15}$$

where

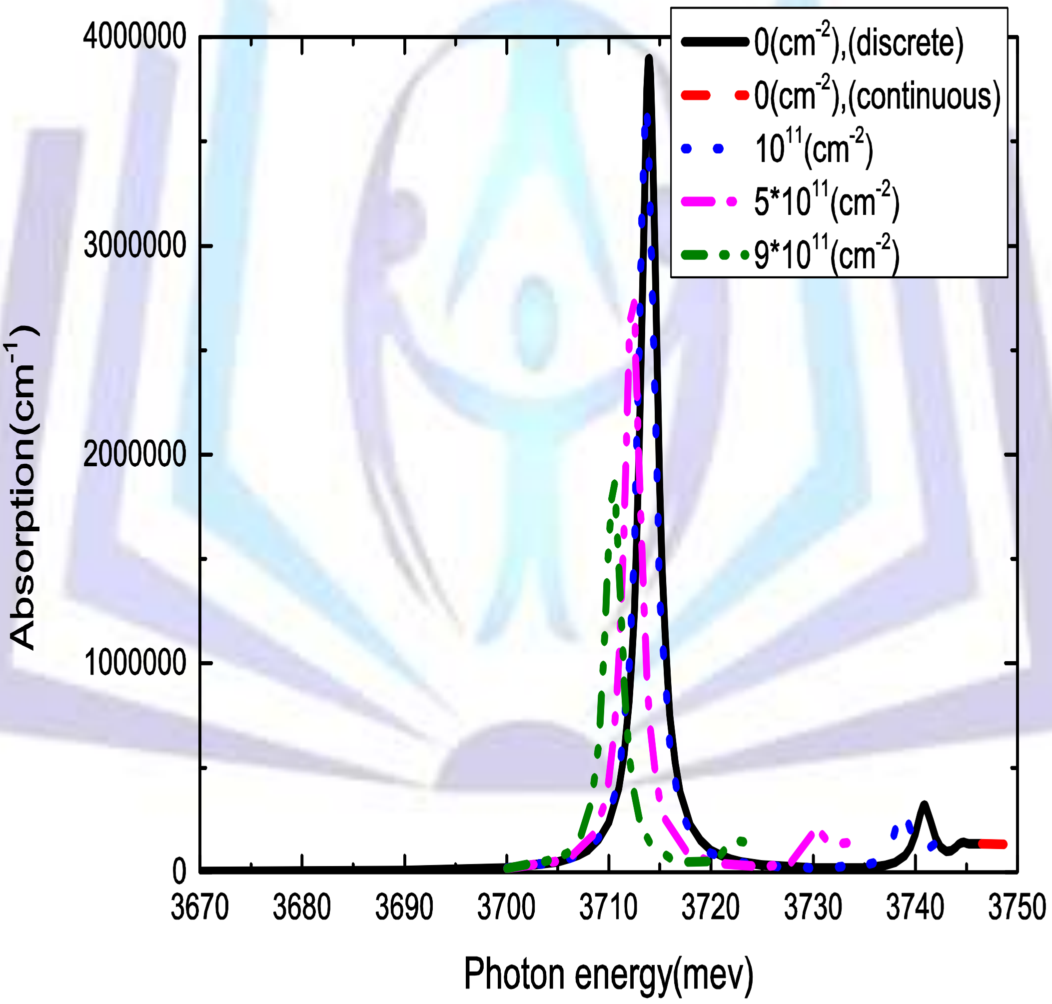

Figure 1: (Color online) Absorption coefficient for the zinc-blende quantum well $GaN/Al_{0.3}Ga_{0.7}N$ with a width 2.6 nm, at a temperature 300 K.

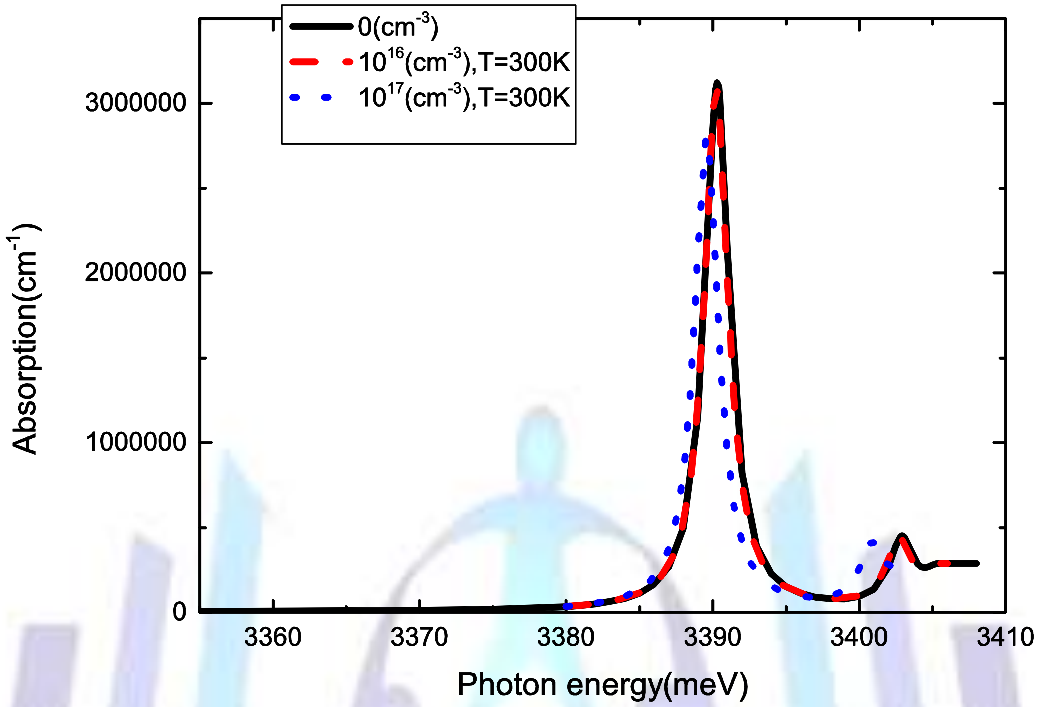

Figure 2: (Color online) Absorption coefficient for zinc-blende bulk crystal GaN.

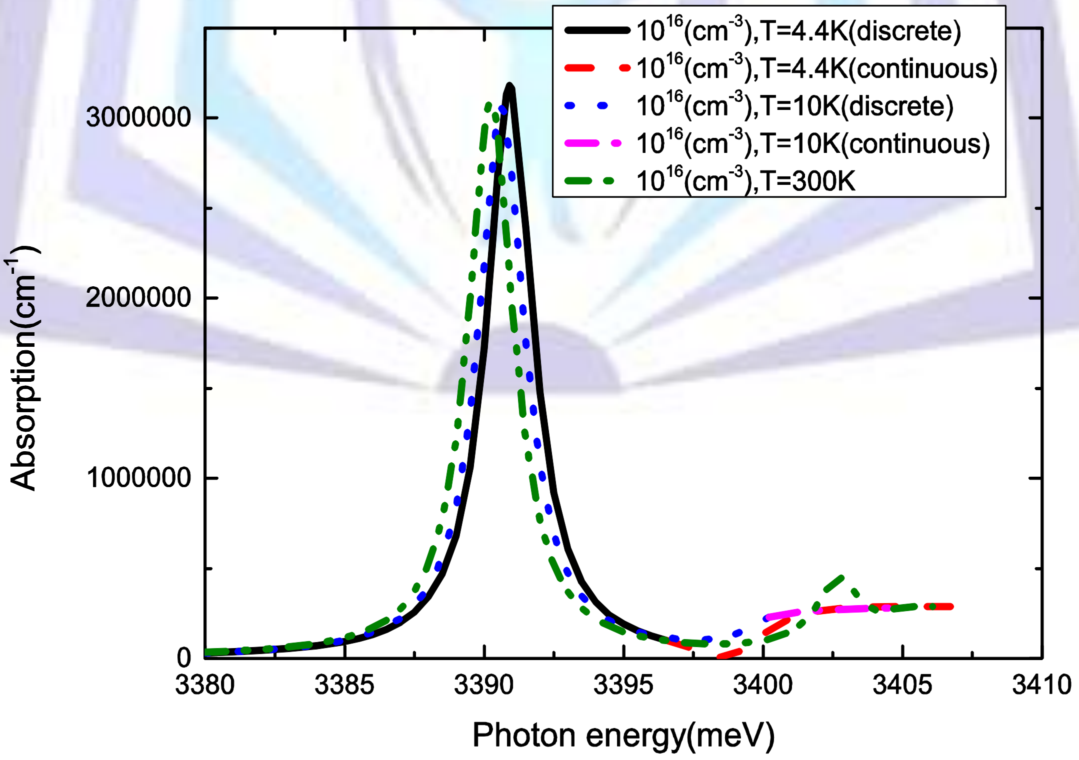

Figure 3: (Color online) Absorption coefficient for zinc-blende bulk crystal GaN.

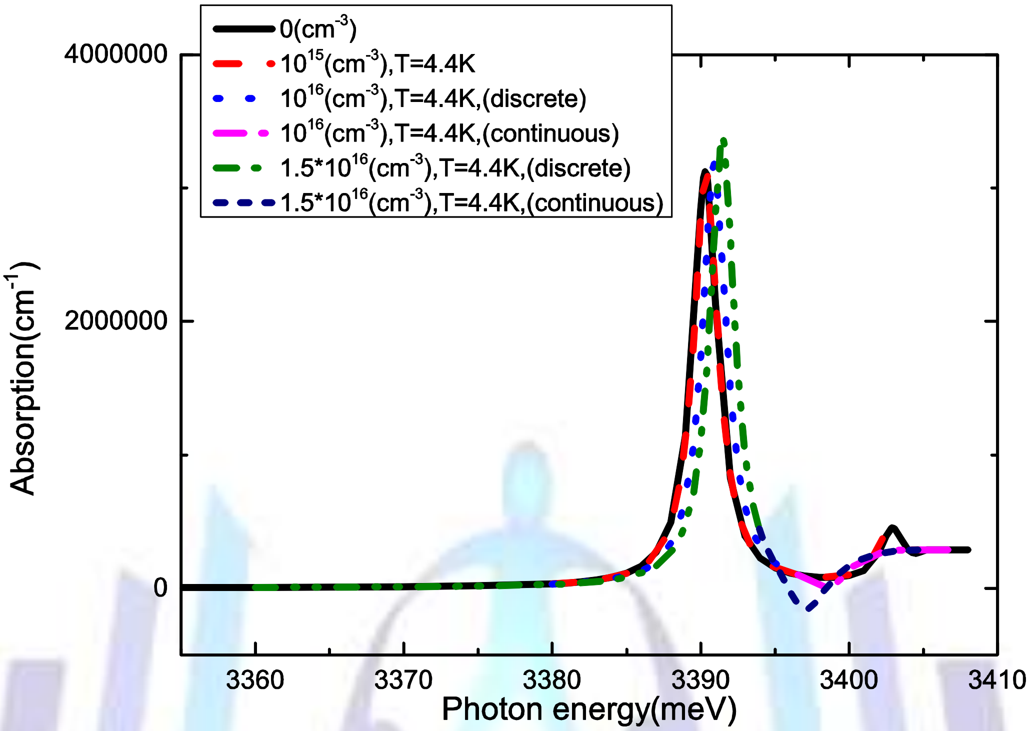

Figure 4: (Color online) Absorption coefficient for zinc-blende bulk crystal GaN.

$$M=\sum_{\mathbf{k}}\frac{n(\varepsilon_{\mathbf{k+q}})-n(\varepsilon_{\mathbf{k}})}{\varepsilon_{\mathbf{k+q}}-\varepsilon_{\mathbf{k}}}. \tag{16}$$

The coefficient of the sum in the second term of series (15) is

$$N\frac{m}{2\hbar^2}\left(\frac{4\pi e^2}{\Omega}\right)^2\frac{\Omega}{(2\pi)^3}\frac{1}{k_{\mathrm{F}}^3}2=$$

$$=N\frac{me^4}{2\hbar^2}\left(\frac{4\pi}{\Omega}\right)^2\frac{\Omega}{(2\pi)^3}\frac{\Omega}{3\pi^2N}2=\frac{me^4}{2\hbar^2}\frac{4}{3\pi^3}, \tag{17}$$

In the third term of the series, the coefficient is

$$\frac{m^2}{2\hbar^4}\left(\frac{4\pi e^2}{\Omega}\right)^3\left(\frac{\Omega}{(2\pi)^3}\right)^2\frac{1}{k_{\mathrm{F}}^3}\frac{1}{k_{\mathrm{F}}}2=\frac{me^4}{2\hbar^2}\frac{4}{3\pi^3}\frac{\alpha r_s}{2\pi^2}.$$

$$\alpha r_s=\frac{me^2}{\hbar^2}\frac{1}{k_{\mathrm{F}}}. \tag{18}$$

Then the series can be rewritten as a infinitely decreasing geometric progression

$$\frac{1}{q^2}-\frac{4}{3\pi^3}\int d^3k\frac{1}{q^4}\frac{n(\varepsilon_{\mathbf{k+q}})-n(\varepsilon_{\mathbf{k}})}{(k+q)^2-k^2}+$$

$$+\frac{4}{3\pi^3}\frac{\alpha r_s}{2\pi^2}\iint d^3k_1d^3k_2\frac{1}{q^6}\frac{n(\varepsilon_{\mathbf{k}_1+\mathbf{q}})-n(\varepsilon_{\mathbf{k}_1})}{(k_1+q)^2-k_1^2}\times$$

$$\times\frac{n(\varepsilon_{\mathbf{k}_2+\mathbf{q}})-n(\varepsilon_{\mathbf{k}_2})}{(k_2+q)^2-k_2^2}-.... \tag{19}$$

By summing all terms of the series, we obtain

$$W_q^{\nu_\alpha\nu_\beta\nu_\beta\nu_\alpha}=\frac{V_q^{\nu_\alpha\nu_\beta\nu_\beta\nu_\alpha}}{\varepsilon_q(N)}. \tag{20}$$

For the dielectric function, we use the static Lindhard formula:

$$\varepsilon_q(N)=1-\sum_{\rho=e,h}\sum_{\nu_\rho}\sum_{\mathbf{p}}V_q^{\nu_\rho\nu_\rho\nu_\rho\nu_\rho}\frac{\hat{n}_{\mathbf{p}+\mathbf{q}}^{\nu_\rho}-\hat{n}_{\mathbf{p}}^{\nu_\rho}}{\varepsilon_{\mathbf{p}+\mathbf{q}}^{\nu_\rho}-\varepsilon_{\mathbf{p}}^{\nu_\rho}}. \tag{21}$$

Since the cyclic diagrams are the basic type of diagrams in the scattering processes at a high density of the electron-hole gas, the diagram method is equivalent of the self-consistency method, as well as the random phase approximation.

The answer how to derive the integro-differential equation (11) for a microscopic dipole is given by the scheme

$$\omega_{\mathbf{p}}^{\nu_e\nu_h}:V_q^{\nu_\alpha\nu_\alpha\nu_\alpha\nu_\alpha}\rightarrow W_q^{\nu_\alpha\nu_\alpha\nu_\alpha\nu_\alpha},n_{\mathbf{p}+\mathbf{q}}^{\nu_\alpha}\rightarrow\Xi_{\mathbf{p}+\mathbf{q},\mathbf{q}}^{\nu_\alpha}, \tag{22}$$

plus the expression, whose graphic representation reminds a binary blister,

$$\sum_{\mathbf{p}}\frac{d\hat{p}_{\mathbf{p}}^{\nu_e\nu_h}}{dt}:V_q^{\nu_e\nu_h\nu_h\nu_e}\rightarrow W_q^{\nu_e\nu_h\nu_h\nu_e},n_{\mathbf{p}}^{\nu_\alpha}\rightarrow\Xi_{\mathbf{p},\mathbf{q}}^{\nu_\alpha}, \tag{23}$$

plus the expression corresponding to the plot in the form of an oyster.

The sum over momenta in the polarization equation, which includes the carrier-carrier correlations of higher orders than Hartree–Fock ones, can be found if the self-energy in the equation is added by the term, which is presented in the equation in the Hartree–Fock approximation, by replacing the Coulomb potential energy with the screened one and the Fermi distribution functions with the $\Xi_{\mathbf{p}+\mathbf{q},\mathbf{q}}^{\nu_\alpha}$ functions, plus the expression, whose schematic representation is in the form of a binary blister. The integro-differential equation should be added by the term which is presented in the equation in the Hartree–Fock approximation, by replacing the Coulomb potential energy with the screened one and the Fermi distribution functions with the $\Xi_{\mathbf{p},\mathbf{q}}^{\nu_\alpha}$ functions, plus the expression, whose schematic representation is in the form of an oyster. We consider the coupled closed diagrams. The sum of all uncoupled diagrams, which include k, closed loops which have $m_1,m_2,...,m_k$ vertices, correspondingly, is the sum of all closed diagrams of the m-th order [30,31].

The absorption spectrums for the zinc-blende GaN/(Al,Ga)N quantum well as well as for the zinc-blende bulk GaN are shown in Figures 1-4 at a temperatures of 300K, 10K, 4.4K if a concentrations or particles in a quantum well are as follows 10^{11} cm $^{-2}$, 5×10^{11} cm $^{-2}$, 9×10^{11} cm $^{-2}$, as well as if a concentrations or particles in a bulk 10^{16} cm $^{-3}$, 10^{17} cm $^{-3}$.

The interesting effects of strong electron-hole Coulomb interaction are presented in these materials. Many-body interactions lead to effects, which consist of the screening, dephasing, bandgap renormalization, and phase-space filling [26-29,32]. It is known [32] the continuum spectra agrees well with Elliot's formula. With increasing free particles concentrations continuum spectra shifts rapidly to lower energies, whereas the energy of lowest exciton remains a constant value. The reason of constant energy of the lowest exciton line consists in compensation of the weakening of the e-h pair binding energy due to screening its of free particles by reduction of edge of absorption (see in Figures 1-4). The cause of this remarkable sight consists in the charge neutrality of an exciton [32].

From Figures 3,4 one can see an arising of negative range at lower wavelength from the lowest exciton line at increasing of particles densities and at constant temperature or at decreasing of temperature at constant of particles densities. Its may be explained by the exchange renormalization of band gap spectra and the Coulomb renormalization of electric dipole momenta. It should be noted that many-particles interactions are of cause the both an arising of negative range at lower wavelength from the lowest exciton line and an disappearance of 2s exciton line. As well as an insignificant enhancement of the lowest exciton is of an arising effect. Our theoretical studies have well agreement with the experimental results [33].

3 Exciton insulator states with "Mexican hat" band structure dispersion

The "Mexican hat" band structure dispersion is found in the form

$$\varepsilon_{\pm} = q^2 \pm \frac{m\Delta}{\hbar^2}\sqrt{1+\frac{4\alpha^2 q^2}{\Delta^2}}, \qquad (24)$$

where $q = \sqrt{q_x^2 + q_y^2}$.

The Schrödinger equation for the calculating of exciton states can be written in the general form

$$(\varepsilon(\mathbf{q}^2) + q_0^2)\Phi(q) = \frac{1}{\pi}\int \frac{\Phi(\mathbf{q}')}{|\mathbf{q}-\mathbf{q}'|}d\mathbf{q}', \qquad (25)$$

where $q_0^2 = -\varepsilon$, ε is a quantized energy. We look for the bound states and hence the energy will be negative.

An integral form of the two-dimensional Schrödinger equation in momentum space for the gapped graphene is solved exactly by projection the two-dimensional space of momentum on the three-dimensional sphere.

For the "Mexican hat" shape band structure dispersion

$$\begin{aligned}\frac{\varepsilon(q^2)+q_0^2}{q^2+q_0^2} = \pm\frac{m\Delta}{4q_0^2\hbar^2}\sqrt{(1-\cos\theta)^2 + \frac{4v_F^2}{\Delta^2}q_0^2(\sin\theta)^2 +} \\ +1,\end{aligned} \qquad (26)$$

where an each point on sphere is defined of two spherical angles θ , ϕ , which are knitted with a momentum q [7,8]. A space angle Ω may be found as surface element on sphere $d\Omega = \sin(\theta)d\theta d\phi = (\frac{2q_0}{q^2+q_0^2})^2 dq$ [7,8]. A spherical angle θ and a momentum q are shown [7,8] to be knitted as

$$\cos\theta = \frac{q^2-q_0^2}{q^2+q_0^2}, \sin\theta = \frac{2qq_0}{q^2+q_0^2}, q^2 = q_0^2(\frac{1+\cos\theta}{1-\cos\theta}). \qquad (27)$$

Using spherical symmetry the solution of integral Schrödinger equation can look for in the form

$$\Phi(q) = \sqrt{q_0}\,(\frac{2q_0}{q^2+q_0^2})^{3/2}\sum_{l=0}^{\infty} A_l Y_l^0(\theta,\phi), \qquad (28)$$

where

$$Y_l^0(\theta,\phi) = \sqrt{\frac{2l+1}{4\pi}}P_l^0(\cos\theta). \qquad (29)$$

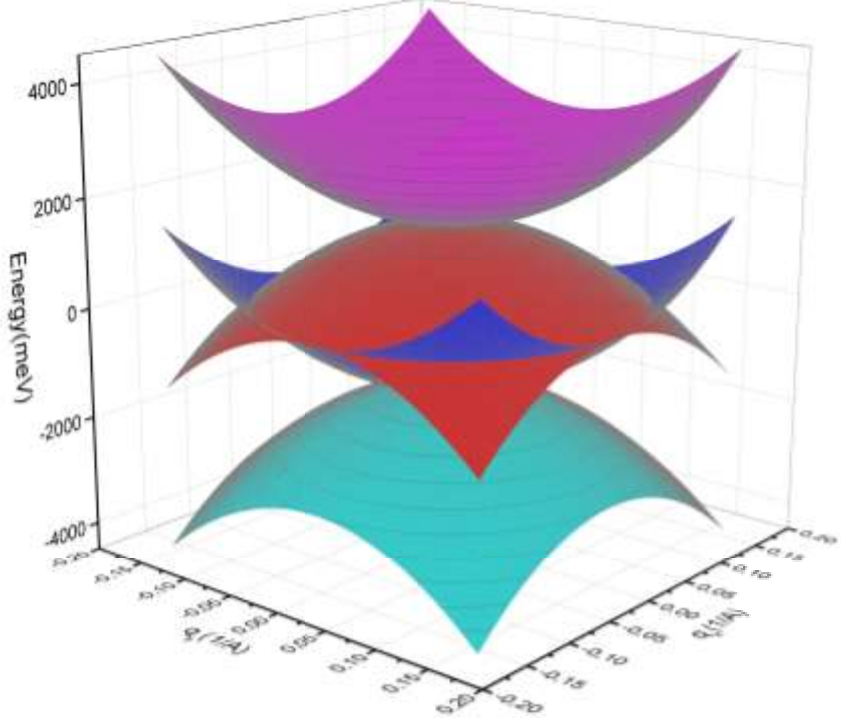

Figure 5: (Color online) "Mexican hat" band spectrum.

Since [7]

$$\frac{(q^2+q_0^2)^{1/2}(q'^2+q_0^2)^{1/2}}{2q_0}\frac{1}{|\mathbf{q}-\mathbf{q}'|}=\sum_{\lambda=0}^{\infty}\sum_{\mu=-\lambda}^{\lambda}\frac{4\pi}{2\lambda+1}Y_\lambda^\mu(\theta,\phi)Y_\lambda^{\mu,*}(\theta',\phi'), \tag{30}$$

then substituting (28), (30) in (25), can find equation

$$\frac{\varepsilon(q^2)+q_0^2}{q^2+q_0^2}\sum_{l=0}^{\infty}A_lY_l^0(\theta,\phi)=\frac{2}{q_0}\sum_{l=0}^{\infty}\sum_{\lambda=0}^{\infty}\sum_{\mu=-\lambda}^{\lambda}\int\frac{1}{2\lambda+1}Y_\lambda^\mu(\theta,\phi)Y_\lambda^{\mu,*}(\theta',\phi')Y_l^0(\theta',\phi')A_l(\frac{2q_0}{q'^2+q_0^2})^2d\mathbf{q}'. \tag{31}$$

The integral equations for "Mexican hat" shape band structure based on Eq. (26) may be found in the form

$$\begin{aligned}&\int(\mp\frac{m\Delta}{4q_0^2\hbar^2}\sqrt{(1-\cos\theta)^2+\frac{4\alpha^2}{\Delta^2}q_0^2(\sin\theta)^2}+1)\sum_{l=0}^{\infty}A_lY_l^0(\theta,\phi)Y_k^{n,*}(\theta,\phi)d\Omega=\\&=\frac{2}{q_0}\int\sum_{\lambda=0}^{\infty}\sum_{\mu=-\lambda}^{\lambda}\sum_{l'=0}^{\infty}\frac{1}{2\lambda+1}Y_\lambda^\mu(\theta,\phi)Y_\lambda^{\mu,*}(\theta',\phi')Y_{l'}^0(\theta',\phi')Y_k^{n,*}(\theta,\phi)d\Omega d\Omega'A_{l'}.\end{aligned} \tag{32}$$

Since [35,36]

$$\cos\theta P_l^m(\cos\theta)=\frac{\sqrt{l^2-m^2}}{\sqrt{4l^2-1}}P_{l-1}^m(\cos\theta)+\frac{\sqrt{(l+1)^2-m^2}}{\sqrt{4(l+1)^2-1}}P_{l+1}^m(\cos\theta), \tag{33}$$

$$\sin\theta P_l^m(\cos\theta)=\frac{\sqrt{(l-m)(l-m-1)}}{\sqrt{4l^2-1}}P_{l-1}^{m+1}(\cos\theta)+\frac{\sqrt{(l+m+1)(l+m+2)}}{\sqrt{4(l+1)^2-1}}P_{l+1}^{m+1}(\cos\theta), \tag{34}$$

then solutions of the integral equation (31) for the energies and wave functions correspondingly can be found analytically with taken into account the normalization condition $(\frac{1}{2\pi})^2 \int \frac{q^2 + q_0^2}{2q_0^2} |\Phi(\mathbf{q})|^2 \ d\mathbf{q} = 1$.

From equation (32) one can obtain the eigenvalue and eigenfunction problem using a condition $\frac{4\alpha^2}{\Delta^2} q_0^2 >> 1$.

The solutions of the quantized series in excitonic Rydbergs where Ry= $m_r e^4/(\varepsilon^2 \hbar^2) = 10.33$ meV, m_r is the reduced mass of an electron-hole pair, and wave functions of the integral equation (32) one can find in the form

$$\varepsilon_l = -\frac{1}{(l + \frac{1}{2})^2}, \tag{35}$$

$$\Phi_l(\cos\theta) = \sqrt{\frac{2\pi}{(q_{0l})^3}} \sum_{n=0}^{\infty} (1 - \cos\theta)^{3/2} P_n^0(\cos\theta), \tag{36}$$

where $q_{0l}^2 = -\varepsilon_l$, $l = 0,1,2,3,4,....$.

Table 1. Quantized spectral series of the excitonic states ε_n, $n = 0,1,2,3,4,....$ in meV, band gap of graphene Δ in meV, effective reduced mass of electron-hole pair m_r, spin-orbit splitting parameter in eV*cm, excitonic Rydberg Ry in meV.

ε_0	ε_1	ε_2	ε_3	Δ	m_r	α	Ry
41.33	4.59	1.65	0.84	1500	0.0335	1.434	10.33

Quantized spectral series of the excitonic states distribute in valence Dirac cone. The energies of bound states are shown to be found as negative, i. e. below of Fermi level. Thus if the electron and hole are separated, their energy is higher than if they are paired.

4 Quantized spectral series of the excitonic states of valence Dirac cone.

In the honeycomb lattice of graphene with two carbon atoms per unit cell the space group is D_{3h}^1 [34]:

D_{3h}^1	$\{E \mid 0\}$	$\{C_3^{(+,-)} \mid 0\}$	$\{C_2'^{(A,B,C)} \mid 0\}$	$\{\sigma_h \mid \tau\}$	$\{S_3^{(-,+)} \mid \tau\}$	$\{\sigma_v^{(A,B,C)} \mid \tau\}$	
K_3^+	2	-1	0	2	-1	0	
g^2	$\{E \mid 0\}$	$\{C_3^{(+,-)} \mid 0\}$	$\{E \mid 0\}$	$\{E \mid 0\}$	$\{S_3^{(-,+)} \mid \tau\}$	$\{E \mid 0\}$	
$\chi^2(g)$	4	1	0	4	1	0	$K_1^+ + K_2^+ + K_3^+$
$\chi(g^2)$	2	-1	2	2	-1	2	
$\frac{1}{2}[\chi^2(g) + \chi(g^2)]$	3	0	1	3	0	1	$K_1^+ + K_3^+$
$\frac{1}{2}\{\chi^2(g) - \chi(g^2)\}$	1	1	-1	1	1	-1	K_2^+

The direct production of two irreducible presentations of wave function and wave vector of difference $\kappa - K$ or $\kappa - K'$ expansion is $K_3^+ \times K_3^{+*}$ and can be expanded on

$$p^{\alpha} : \tau_{\psi} \times \tau_k = (K_1^+ + K_2^+ + K_3^+) \times K_3^+ = K_3^+ \times K_3^+. \qquad (37)$$

In the low-energy limit the single-particle spectrum is Dirac cone described by the massless Dirac equation for a massless Dirac fermions (Majorana fermions). The Hamiltonian of graphene for a massless Dirac fermions [6]

$$\hat{H} = v_F (\tau q_x \hat{\sigma}_x + q_y \hat{\sigma}_y), \qquad (38)$$

where q_x, q_y are Cartesian components of a wave vector, $\tau = \pm 1$ is the valley index, $v_F = 10^6$ m/s is the graphene Fermi velocity, $\hat{\sigma}_x$, $\hat{\sigma}_y$ are Pauli matrices (here we assume that $\hbar = 1$).

The dispersion of energy bands may be found in the form [6]

$$\varepsilon_{\pm} = \pm v_F q, \qquad (39)$$

where $q = \sqrt{q_x^2 + q_y^2}$.

The Schrödinger equation for the calculating of exciton states can be written in the general form

$$(\varepsilon(q) + q_0^2)\Phi(\mathbf{q}) = \frac{1}{\pi} \int \frac{\Phi(\mathbf{q}')}{|\mathbf{q} - \mathbf{q}'|} d\mathbf{q}', \qquad (40)$$

where $q_0^2 = -\varepsilon$, ε is a quantized energy. We look for the bound states and hence the energy will be negative.

For the single layer graphene

$$\frac{\varepsilon(q) + q_0^2}{q^2 + q_0^2} = \pm \frac{v_F}{2q_0} \sin(\theta) + \frac{1 - \cos\theta}{2}. \qquad (41)$$

An integral form of the two-dimensional Schrödinger equation in momentum space for the graphene is solved exactly by projection the two-dimensional space of momentum on the three-dimensional sphere.

When an each point on sphere is defined of two spherical angles θ, ϕ, which are knitted with a momentum $\mathbf{q}$ [7,8]. A space angle Ω may be found as surface element on sphere $d\Omega = \sin(\theta) d\theta d\phi = (\frac{2q_0}{q^2 + q_0^2})^2 d\mathbf{q}$ [7,8]. A spherical angle θ and a momentum q are shown [7,8] to be knitted as

$$\cos\theta = \frac{q^2 - q_0^2}{q^2 + q_0^2}, \sin\theta = \frac{2qq_0}{q^2 + q_0^2}, q^2 = q_0^2 (\frac{1 + \cos\theta}{1 - \cos\theta}). \qquad (42)$$

Using spherical symmetry the solution of integral Schrödinger equation can look for in the form

$$\Phi(\mathbf{q}) = \sqrt{q_0} (\frac{2q_0}{q^2 + q_0^2})^{3/2} \sum_{l=0}^{\infty} A_l Y_l^0 (\theta, \phi), \qquad (43)$$

where

$$Y_l^0 (\theta, \phi) = \sqrt{\frac{2l + 1}{4\pi}} P_l^0 (\cos\theta). \qquad (44)$$

Since [7]

$$\frac{(q^2 + q_0^2)^{1/2} (q'^2 + q_0^2)^{1/2}}{2q_0} \frac{1}{|\mathbf{q} - \mathbf{q}'|} = \sum_{\lambda=0}^{\infty} \sum_{\mu=-\lambda}^{\lambda} \frac{4\pi}{2\lambda + 1} Y_{\lambda}^{\mu} (\theta, \phi) Y_{\lambda}^{\mu,*} (\theta', \phi'), \qquad (45)$$

then substituting (43), (45) in (40), one can find equation

$$\frac{\varepsilon(q)+q_0^2}{q^2+q_0^2}\sum_{l=0}^{\infty}A_l Y_l^0(\theta,\phi)=\frac{2}{q_0}\sum_{l=0}^{\infty}\sum_{\lambda=0}^{\infty}\sum_{\mu=-\lambda}^{\lambda}\int\frac{1}{2\lambda+1}Y_\lambda^\mu(\theta,\phi)Y_\lambda^{\mu,*}(\theta',\phi')Y_l^0(\theta',\phi')A_l\left(\frac{2q_0}{q'^2+q_0^2}\right)^2 d\mathbf{q}'. \quad (46)$$

The integral equations for SLG based on Eq. (41) may be found in the form

$$\int\left(\pm\frac{v_F}{2q_0}\sin(\theta)+\frac{1-\cos\theta}{2}\right)\sum_{l=0}^{\infty}A_l Y_l^0(\theta,\phi)Y_k^{n,*}(\theta,\phi)d\Omega=$$
$$=\frac{2}{q_0}\int\sum_{\lambda=0}^{\infty}\sum_{\mu=-\lambda}^{\lambda}\sum_{l'=0}^{\infty}\frac{1}{2\lambda+1}Y_\lambda^\mu(\theta,\phi)Y_\lambda^{\mu,*}(\theta',\phi')Y_{l'}^0(\theta',\phi')Y_k^{n,*}(\theta,\phi)d\Omega d\Omega' A_{l'}. \quad (47)$$

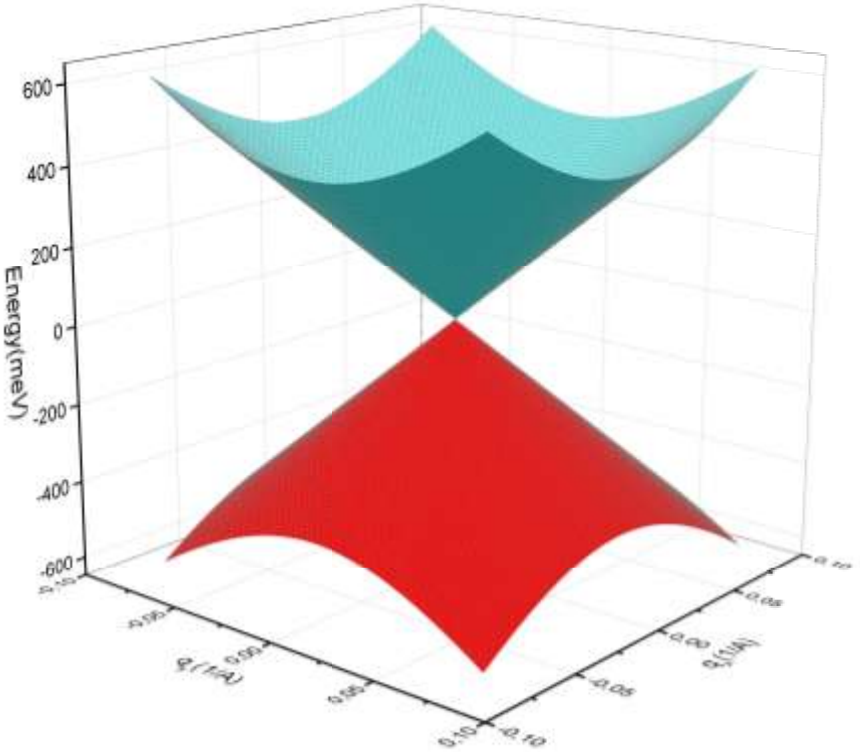

Figure 6: (Color online) Single-particle spectrum of graphene for massless Dirac fermions (Majorana fermions).

Since [35,36]

$$\cos\theta P_l^m(\cos\theta)=\frac{\sqrt{l^2-m^2}}{\sqrt{4l^2-1}}P_{l-1}^m(\cos\theta)+\frac{\sqrt{(l+1)^2-m^2}}{\sqrt{4(l+1)^2-1}}P_{l+1}^m(\cos\theta), \quad (48)$$

$$\sin\theta P_l^m(\cos\theta)=\frac{\sqrt{(l-m)(l-m-1)}}{\sqrt{4l^2-1}}P_{l-1}^{m+1}(\cos\theta)+\frac{\sqrt{(l+m+1)(l+m+2)}}{\sqrt{4(l+1)^2-1}}P_{l+1}^{m+1}(\cos\theta), \quad (49)$$

then solutions of the integral equation (46) for the energies and wave functions correspondingly can be found analytically with taken into account the normalization condition $\left(\frac{1}{2\pi}\right)^2\int\frac{q^2+q_0^2}{2q_0^2}|\Phi(\mathbf{q})|^2\ d\mathbf{q}=1$.

From equation (47) one can obtain the eigenvalue and eigenfunction problem one can find recurrence relation

$$\frac{1}{2}(l+\frac{1}{2})A_l+\frac{1}{q_0}A_l+\frac{1}{2}A_{l-1}(l+\frac{1}{2})a_l+\frac{1}{2}A_{l+1}(l+\frac{1}{2})b_l=0. \tag{50}$$

The solutions of the quantized series in excitonic Rydbergs where Ry=87.37 meV, and wave functions of the integral equation (47) one can find in the form

$$\varepsilon_0=-\frac{1}{(\frac{1}{4}+\frac{1}{2}(1+\frac{1}{2})a_1)^2}, \tag{51}$$

$$\varepsilon_1=-\frac{1}{(\frac{1}{2}(1+\frac{1}{2})+\frac{1}{4}b_0+\frac{1}{2}(2+\frac{1}{2})a_2)^2}, \tag{52}$$

$$\varepsilon_2=-\frac{1}{(\frac{1}{2}(2+\frac{1}{2})+\frac{1}{2}(1+\frac{1}{2})b_1+\frac{1}{2}(3+\frac{1}{2})a_3)^2}, \tag{53}$$

$$\varepsilon_3=-\frac{1}{(\frac{1}{2}(3+\frac{1}{2})+\frac{1}{2}(2+\frac{1}{2})b_2+\frac{1}{2}(4+\frac{1}{2})a_4)^2}, \tag{54}$$

$$\Phi_l(\cos\theta)=\sqrt{\frac{2\pi}{(q_{0l})^3}}\sum_{n=0}^{\infty}(1-\cos\theta)^{3/2}P_n^0(\cos\theta), \tag{55}$$

where $q_{0l}^2=-\varepsilon_l$, $l=0,1,2,3,4,....$,

$$a_l=\frac{1}{2\pi}\sqrt{\frac{2(l-1)+1}{2}}\sqrt{\frac{2}{2l+1}}\frac{l}{\sqrt{4l^2+1}}, \tag{56}$$

$$b_l=\frac{1}{4\pi}\sqrt{2(l+1)+1}\sqrt{2l+1}\frac{l+1}{\sqrt{4(l+1)^2-1}}. \tag{57}$$

Table 2. Quantized spectral series of the excitonic states which distribute in valence cone ε_n,

ε_0	ε_1	ε_2	ε_3	Ry
1107.94	122.47	39.59	17.97	87.37

$n=0,1,2,3,...$ **in meV, exciton Rydberg Ry in meV.**

Quantized spectral series of the excitonic states distribute in valence Dirac cone. The energies of bound states are shown to be found as negative, i. e. below of Fermi level. Thus if the electron and hole are separated, their energy is higher than if they are paired.

4.1 Elliott formula and light absorption rates of the excitonic states of valence Dirac cone.

The intervalley transitions probability caused intervalley photoexcitations taken into account Coulomb interaction of electron-hole pair one can obtain from Fermi golden rule in the form

$$\begin{aligned} P = \frac{2\pi}{\hbar}\left(\frac{ev_F E_\omega}{\hbar\omega}\right)^2 \sum_n \Big(\sum_{\mathbf{q}} |\langle \pm 1, \mathbf{q} | \hat{\sigma}_{x,y} | \mp 1, \mathbf{q}\rangle| \times \\ \times \Phi_n\left(\frac{q^2 - q_0^2}{q^2 + q_0^2}\right)\Big)^2 [\delta_\gamma(\varepsilon_n - \hbar\omega) + \delta_\gamma(\varepsilon_n + \hbar\omega)]. \end{aligned} \tag{58}$$

Considering the case of relatively weak excitation the total rate of increase of the number of photons in the fixed mode one can obtain in the form

$$\begin{aligned} R = \frac{2\pi}{\hbar}\left(\frac{ev_F E_\omega}{\hbar\omega}\right)^2 \sum_n \Big(\sum_{q} |\langle \pm 1, q | \hat{\sigma}_{x,y} | \mp 1, q\rangle| \times \\ \times \Phi_n\left(\frac{q^2 - q_0^2}{q^2 + q_0^2}\right)\Big)^2 [\delta_\gamma(\varepsilon_n - \hbar\omega) + \delta_\gamma(\varepsilon_n + \hbar\omega)]. \end{aligned} \tag{59}$$

The change in the energy density of electromagnetic waves can be presented in the form

$$\frac{dW}{dt} = \frac{\hbar\omega}{S} R. \tag{60}$$

Under ac electric field $E_\omega \mathbf{e}\cos(qz - \omega t)$ the energy density of electromagnetic waves one can obtain in the form $W = \frac{1}{8\pi}\kappa E_\omega^2$. Light absorption rate one can obtain in the form $\alpha(\omega) = \frac{1}{W}\frac{dW}{dz}$. Since $\frac{dW}{dz} = \frac{dW}{dt}\frac{\sqrt{\kappa}}{c}$ then light absorption rate with taken into account $|\langle \pm 1, \mathbf{q} | \hat{\sigma}_{x,y} | \mp 1, \mathbf{q}\rangle|^2 = 1/2$ can be rewritten in the form

$$\begin{aligned} \Im(\alpha(\omega)) = \frac{16}{\sqrt{\kappa} c \hbar^2 \omega}(ev_F)^2 \sum_n \Big(\int d\mathbf{q} \times \\ \times \Phi_n\left(\frac{q^2 - q_0^2}{q^2 + q_0^2}\right)\Big)^2 [\delta_\gamma(\varepsilon_n - \hbar\omega) + \delta_\gamma(\varepsilon_n + \hbar\omega)], \end{aligned} \tag{61}$$

where $\sum_{\mathbf{q}} \to \frac{S}{(2\pi)^2}\int d\mathbf{q}$ in a formula (59).

Table 3. Light absorption rate of quantized spectral series of the excitonic states which distribute in valence cone α_n, $n = 0,1,...$ in cm $^{-1}$.

α_0	α_1
$7.67*10^{22}$	$1.14*10^{25}$

5 Results and discussions

The integral Schrödinger equation for a parabolic bands was analytically solved by the projection the three-dimensional momentum space onto the surface of a four-dimensional unit sphere by Fock in 1935 [8]. In integral form of the two-dimensional Schrödinger equation of Kepler problem in momentum space is solved exactly by the projection of the two-dimensional space of momentum on the three-dimensional sphere in the paper [7].

In graphene the existing of bound pair states are still subject matter of researches [13].

In the paper [37,38] the possibility of extremum loop or toroidal energy surfaces in würtzite semiconductor is discussed. The Bychkov-Rashba model [39] describes the electron motion in two-dimensional system with applied electric potential gradient field perpendicularly to the plane of system.

This Rashba spin splitting causes the shifting of oppositely spin-polarized energy band by momentum q in opposite directions.

The Rashba and Dresselhaus spin-orbit couplings in GaAs quantum wells were studies in the paper [40].

The bismuth tellurohalides BiTeCl, BiTeBr and BiTeI have hexagonal crystal structures and giant Rashba spin splitting in two-dimensional systems [41,42]. These materials in the low-energy limit are described "Mexican hat" shape dispersion.

In the paper an integral two-dimensional Schrödinger equation of the electron-hole pairing for particles with complex dispersion is analytically solved. A complex dispersions lead to fundamental difference in exciton insulator states and their wave functions.

We analytically solve an integral two-dimensional Schrödinger equation of the electron-hole pairing for particles with electron-hole symmetry of reflection.

It is known that the Coulomb interaction leads to the semimetal-exciton insulator transition, where gap is opened by particle-particle exchange interaction [12]. The perfect host combines a small gap and a large exciton binding energy [12].

We consider the pairing between oppositely charged particles in a materials with "Mexican hat" shape band structure dispersion or in materials with giant Rashba spin splitting and in graphene. The Coulomb interaction leads to the electron-hole bound states scrutiny study of which acquire significant attention in explanations of hight-temperature superconductivity.

It is known [9,12] if the exciton binding energy is greater than the flat band gap in narrow-gap semiconductor or semimetal then at sufficiently low temperature the insulator ground state is instable concerning to the exciton formation with follow up spontaneous production of excitons. In a system undergo a phase transition into a exciton insulator phase similarly to BCS superconductor. In a semiconductors with "Mexican hat" shape band structure dispersion as well as in graphene the electron-hole pairing leads to exciton insulator states.

The integral Schrödinger equation for a parabolic bands was analytically solved by the projection the three-dimensional momentum space onto the surface of a four-dimensional unit sphere by Fock in 1935 [8].

In the paper an integral two-dimensional Schrödinger equation of the electron-hole pairing for particles with complex dispersion is analytically solved. A complex dispersion leads to fundamental difference in the energy of exciton insulator states and their wave functions.

We analytically solve an integral two-dimensional Schrödinger equation of the electron-hole pairing for particles with electron-hole symmetry of reflection.

It is known that the Coulomb interaction leads to the semimetal-exciton insulator transition, where gap is opened by electron-electron exchange interaction [9,16-18]. The perfect host combines a small gap and a large exciton binding energy [9,12].

The particle-hole symmetry of Dirac equation of layered materials allows perfect pairing between electron Fermi sphere and hole Fermi sphere in the valence band and conduction band and hence driving the Cooper instability. In the weak-coupling limit in graphene with the occupied conduction-band states and empty valence-band states inside identical Fermi surfaces in band structure, the exciton condensation is a consequence of the Cooper instability.

It is shown that the solutions of Coulomb problem of electron-hole pair does not depend from a width of band gap of graphene. It means the absolute compliance with the cyclic geometry of diagrams at justification of the equation of motion for a microscopic dipole of graphene where $r_s > 1$.

6 Conclusions

In this paper we found the solution the integral Schrödinger equation in a momentum space of two interacting via a Coulomb potential Dirac particles that form the exciton in graphene and in materials with "Mexican hat" band structure dispersion as well as in zinc-blende GaN.

In low-energy limit this problem is solved analytically. We obtained the energy dispersion and wave function of the exciton in graphene and in materials with "Mexican hat" band structure dispersion as well as in zinc-blende GaN. The excitons were considered as a system of two oppositely charge Dirac particles interacting via a Coulomb potential.

We solve this problem in a momentum space because on the whole the center-of-mass and the relative motion of the two Dirac particles can not be separated.

We analytically solve an integral two-dimensional Schrödinger equation of the electron-hole pairing for particles with electron-hole symmetry of reflection. An integral form of the two-dimensional Schrödinger equation in momentum space for graphene and in materials with "Mexican hat" band structure dispersion is solved exactly by projection the two-dimensional space of momentum on the three-dimensional sphere.

Quantized spectral series of the excitonic states distribute in valence Dirac cone. The energies of bound states are shown to be found as negative, i. e. below of Fermi level. Thus if the electron and hole are separated, their energy is higher than if they are paired. In the SLG as well as in materials with "Mexican hat" band structure dispersion the electron-hole pairing leads to the exciton insulator states.

It is shown that the solutions of Coulomb problem of electron-hole pair does not depend from a width of band gap of graphene. It means the absolute compliance with the cyclic geometry of diagrams at justification of the equation of motion for a microscopic dipole of graphene where $r_s > 1$.

Appendix A

D_{3h}^1	$\{E\|0\}$	$\{C_3^{(+,-)}\|0$	$\{C_2'^{(A,B,C)}\|($	$\{\sigma_h\|\tau\}$	$\{S_3^{(-,+)}\|\tau\}$	$\{\sigma_v^{(A,B,C)}\|\tau\}$	
K_1^+	1	1	1	1	1	1	x^2+y^2, z^2
K_2^+	1	1	-1	1	1	-1	J_z
K_3^+	2	-1	0	2	-1	0	(x, y)
K_1^-	1	1	1	-1	-1	-1	
K_2^-	1	1	-1	-1	-1	1	z
K_3^-	2	-1	0	-2	1	0	(x^2-y^2, xy), (J_x, J_y)

Appendix B

From a trigonometric calculations one can find a following recurrence relations

$$\cot\theta P_l^{m+1}(\cos\theta) = \frac{P_l^{m+2}(\cos\theta) + [l(l+1) - m(m+1)]P_l^m(\cos\theta)}{2(m+1)}, \quad (62)$$

$$\frac{1}{\sin\theta} P_{l-1}^m(\cos\theta) = \frac{(2l+1)P_l^{m+1}(\cos\theta) + (l-m)(l-m+1)(2l+1)P_l^{m-1}(\cos\theta)}{((l+m)(l+m+1) - (l-m)(l-m+1))}, \quad (63)$$

$$\cot\theta P_l^m(\cos 2\theta) = (\frac{1}{\sin 2\theta} + \cot 2\theta)P_l^m(\cos 2\theta), \quad (64)$$

$$(\frac{1}{2}(3 + 4(\cot\theta)^2) - \frac{1}{2} - \frac{1}{\sin\theta})P_l^m(\cos 2\theta) = \cot\theta P_l^m(\cos 2\theta), \quad (65)$$

where

$$P_l^m(x) = \frac{1}{2^m}\frac{(l+m)!}{(l-m)!m!}(1-x^2)^{m/2} F(m-l, m+l+1, m+1, \frac{1-x}{2}), \quad (66)$$

$$F(\alpha,\beta,\gamma,z) = -\frac{1}{2\pi i}\frac{\Gamma(1-\alpha)\Gamma(\gamma)}{\Gamma(\gamma-\alpha)}\oint(-t)^{\alpha-1}(1-t)^{\gamma-\alpha-1}(1-tz)^{-\beta}dt. \quad (67)$$

In order to find a light absorption rates necessarily to solve the integral

$$J = \int_{-1}^{1} dx F(-l, l+1, 1, \frac{1-x}{2}). \quad (68)$$

Substituting (67) into (68) we obtain the integral in the form

$$J=-\frac{1}{2\pi i}\frac{\Gamma(1+l)\Gamma(1)}{\Gamma(1+l)}\int_{-1}^{1}dx\oint(-t)^{-l-1}(1-t)^{l}(1-\frac{t}{2}+\frac{tx}{2})^{-l-1}dt, \tag{69}$$

which can be rewritten as follows

$$J=-\frac{1}{2\pi i}\frac{\Gamma(1+l)\Gamma(1)}{\Gamma(1+l)}\int_{-1}^{1}dx\oint(-t)^{-l-1}(1-t)^{l}(1-\frac{t}{2})^{-l-1}(1+\frac{tx}{2-t})^{-l-1}dt. \tag{70}$$

The solution the following integral

$$J=\int_{-1}^{1}(1+\frac{tx}{2-t})^{-l-1}dx, \tag{71}$$

may be found by substitution

$$y=\frac{tx}{2-t}. \tag{72}$$

We find the solution of the integral

$$J=\int_{-\frac{t}{2-t}}^{\frac{t}{2-t}}(1+y)^{-l-1}dy=-\frac{2^{-l}}{l+2}(2-t)^{l}+\frac{2^{-l}}{l+2}(1-t)^{-l}(2-t)^{l}. \tag{73}$$

Then substituting (73) into (70) we obtain the integral in the form

$$J=-\frac{1}{2\pi i}\frac{\Gamma(1+l)\Gamma(1)}{\Gamma(1+l)}\frac{2^{-l}}{l+2}(\oint(-t)^{-l-1}(1-t)^{l}(1-\frac{t}{2})^{-1}dt-\oint(-t)^{-l-1}(1-t)^{0}(1-\frac{t}{2})^{-1}dt)2^{l}, \tag{74}$$

which can be expressed via a hypergeometric functions as follows

$$J=\frac{\Gamma(1)}{l+2}(F(-l,1,1,\frac{1}{2})\frac{1}{\Gamma(1)}-F(-l,1,-l,\frac{1}{2})\frac{\Gamma(1)}{\Gamma(1+l)\Gamma(-l)}). \tag{75}$$

In a similar form can be calculated the integral

$$J=\int_{-1}^{1}dxP_{l}^{m}(x). \tag{76}$$

Substituting (66) into (76) we obtain the integral in the form

$$J=\int_{-1}^{1}dx\frac{1}{2^{m}}\frac{(l+m)!}{(l-m)!m!}(1-x^{2})^{m/2}F(m-l,m+l+1,m+1,\frac{1-x}{2}). \tag{77}$$

Using the formula (67) the integral (77) one can transform into the integral

$$J=-\frac{1}{2\pi i}\frac{\Gamma(1-m+l)\Gamma(m+1)}{\Gamma(1+l)}\frac{1}{2^{m}}\frac{(l+m)!}{(l-m)!m!}\int_{-1}^{1}dx(1-x^{2})^{m/2}\oint(-t)^{m-l-1}(1-t)^{l}(1-t\frac{1-x}{2})^{-m-l-1}dt, \tag{78}$$

which can be rewritten in the form

$$J=-\frac{1}{2\pi i}\frac{\Gamma(1-m+l)\Gamma(m+1)}{\Gamma(1+l)}\frac{1}{2^{m}}\frac{(l+m)!}{(l-m)!m!}\int_{-1}^{1}dx(1-x^{2})^{m/2}\oint(-t)^{m-l-1}(1-t)^{l}(1-\frac{t}{2})^{-m-l-1}(1+\frac{tx}{2-t})^{-m-l-1}dt. \tag{79}$$

In order to find the solution of the integral (79) it is necessarily to consider the integral of form:

$$J = \int_{-1}^{1} (1-x^2)^{m/2} (1+\frac{tx}{2-t})^{-m-l-1} dx, \tag{80}$$

which can be transformed into the integral of form:

$$J = (\frac{t}{2-t})^{-m-l-1} \int_{-1}^{1} (1-x^2)^{m/2} (\frac{2-t}{t}+x)^{-m-l-1} dx. \tag{81}$$

The solution the integral (108) one can find using the binomial theorem and following replacements

$$J = (\frac{t}{2-t})^{-m-l-1} \int_{-1}^{1} \sum_{k=0}^{\gamma} \frac{\gamma!}{k!(\gamma-k)!} (1)^{\gamma-k} (-1)^k x^{2k} (\frac{2-t}{t}+x)^{-m-l-1} dx, \tag{82}$$

$$\gamma = m/2\,,$$

$$u = (\frac{\frac{2-t}{t}+x}{x})^{-1/(m+l+1)}. \tag{83}$$

So integral (82) may be rewritten as follows

$$J = (\frac{2-t}{t})^{2k-m-l-1} \int u^{2(m+l+1)(k+1)-(m+l+1)^2-(m+l+1)} (1-u^{(m+l+1)})^{-2(k+1)+m+l+1} du. \tag{84}$$

The solution of the integral (111) one can find by replacement

$$u = (y)^{1/(m+l+1)}. \tag{85}$$

We obtain the following expression for the sought for integral:

$$\begin{aligned} J &= \frac{1}{(m+l+1)} (\frac{2-t}{t})^{2k-m-l-1} \int_{-t/(2-2t)}^{t/2} y^{2(k+1)-m-l-3+\frac{1}{m+l+1}} (1-y)^{-2(k+1)+m+l+1} dy = \\ &= \frac{1}{(m+l+1)} (\frac{2-t}{t})^{2k-m-l-1} \int_{-t/(2-2t)}^{t/2} y^{2(k+1)-m-l-3+\frac{1}{m+l+1}} \times \\ &\times \sum_{n=0}^{-2k+m+l-1} \frac{(-2k+m+l-1)!}{(n)!(-2k+m+l-1-n)!} (1)^{(-2k+m+l-1-n)} (-y)^n dy. \end{aligned} \tag{86}$$

The solution the integral (86) one can find using the binomial theorem

$$(1-y)^{-2(k+1)+m+l+1} = \sum_{n=0}^{-2k+m+l-1} \frac{(-2k+m+l-1)!}{(n)!(-2k+m+l-1-n)!} (1)^{(-2k+m+l-1-n)} (-y)^n. \tag{87}$$

Substituting equation (87) in the integral (86) one can obtain the sought for integral in the form

$$\begin{aligned} J = \frac{1}{(m+l+1)} (\frac{2-t}{t})^{2k-m-l-1} \sum_{n=0}^{-2k+m+l-1} \frac{(-2k+m+l-1)!}{(n)!(-2k+m+l-1-n)!} (1)^{(-2k+m+l-1-n)} (-1)^n \times \\ \times \int_{-t/(2-2t)}^{t/2} y^{2(k+1)-m-l-3+\frac{1}{m+l+1}+n} dy. \end{aligned} \tag{88}$$

We find the solution of the integral (88) in the form:

$$J = \frac{1}{(m+l+1)}\left(\frac{2-t}{t}\right)^{2k-m-l-1}\sum_{n=0}^{-2k+m+l-1}\frac{(-2k+m+l-1)!}{(n)!(-2k+m+l-1-n)!}(1)^{(-2k+m+l-1-n)}(-1)^n\times$$
$$\times\frac{y^{2k-m-l+\frac{1}{m+l+1}+n}}{(2k-m-l+\frac{1}{m+l+1}+n)}\Big|_{-t/(2-2t)}^{t/2}. \qquad (89)$$

Substituting (89) in (82) one can rewrite the integral (82) in the form:

$$J = \left(\frac{t}{2-t}\right)^{-m-l-1}\sum_{k=0}^{\gamma}\frac{\gamma!}{k!(\gamma-k)!}(1)^{\gamma-k}(-1)^k\times$$
$$\times\frac{1}{(m+l+1)}\left(\frac{2-t}{t}\right)^{2k-m-l-1}\sum_{n=0}^{-2k+m+l-1}\frac{(-2k+m+l-1)!}{(n)!(-2k+m+l-1-n)!}(1)^{(-2k+m+l-1-n)}(-1)^n\times \qquad (90)$$
$$\times\frac{y^{2k-m-l+\frac{1}{m+l+1}+n}}{(2k-m-l+\frac{1}{m+l+1}+n)}\Big|_{-t/(2-2t)}^{t/2}.$$

Substituting (90) in the sought for integral (89) one can rewrite the integral (89) as follows:

$$J = -\frac{1}{2\pi i}\frac{\Gamma(1-m+l)\Gamma(m+1)}{\Gamma(1+l)}\frac{1}{2^m}\frac{(l+m)!}{(l-m)!m!}\frac{1}{(m+l+1)}\sum_{k=0}^{\gamma}\frac{\gamma!}{k!(\gamma-k)!}(1)^{\gamma-k}(-1)^k\times$$
$$\times\sum_{n=0}^{-2k+m+l-1}\frac{(-2k+m+l-1)!}{(n)!(-2k+m+l-1-n)!}(1)^{(-2k+m+l-1-n)}(-1)^n\times$$
$$\times\sum_{s=0}^{2k}\frac{(2k)!}{(s)!(2k-s)!}(-1)^s\times \qquad (91)$$
$$\times\oint(-t)^{m-l-1}(1-t)^l\left(1-\frac{t}{2}\right)^{-m-l-1}\times$$
$$\times\left(\frac{2}{t}\right)^{(2k-s)}\frac{y^{2k-m-l+\frac{1}{m+l+1}+n}}{(2k-m-l+\frac{1}{m+l+1}+n)}\Big|_{-t/(2-2t)}^{t/2}dt,$$

which can be rewritten in the form

$$J = -\frac{1}{2\pi i}\frac{\Gamma(1-m+l)\Gamma(m+1)}{\Gamma(1+l)}\frac{1}{2^m}\frac{(l+m)!}{(l-m)!m!}\frac{1}{(m+l+1)}\sum_{k=0}^{\gamma}\frac{\gamma!}{k!(\gamma-k)!}(1)^{\gamma-k}(-1)^k\times$$
$$\times\sum_{n=0}^{-2k+m+l-1}\frac{(-2k+m+l-1)!}{(n)!(-2k+m+l-1-n)!}(1)^{(-2k+m+l-1-n)}(-1)^n\times$$
$$\times\sum_{s=0}^{2k}\frac{(2k)!}{(s)!(2k-s)!}(-1)^s\times \qquad (92)$$
$$\times\frac{1}{(2k-m-l+\frac{1}{m+l+1}+n)}\oint(-t)^{m-l-1}(1-t)^l\left(1-\frac{t}{2}\right)^{-m-l-1}\times$$
$$\times\left(\frac{2}{t}\right)^{(2k-s)}\left((t/2)^{2k-m-l+\frac{1}{m+l+1}+n}-(-t/(2-2t))^{2k-m-l+\frac{1}{m+l+1}+n}\right)dt,$$

or as follows

$$\begin{aligned}J=&-\frac{1}{2\pi i}\frac{\Gamma(1-m+l)\Gamma(m+1)}{\Gamma(1+l)}\frac{1}{2^m}\frac{(l+m)!}{(l-m)!m!}\frac{1}{(m+l+1)}\sum_{k=0}^{\gamma}\frac{\gamma!}{k!(\gamma-k)!}(1)^{\gamma-k}(-1)^k\times\\&\times\sum_{n=0}^{-2k+m+l-1}\frac{(-2k+m+l-1)!}{(n)!(-2k+m+l-1-n)!}(1)^{(-2k+m+l-1-n)}(-1)^n\times\\&\times\sum_{s=0}^{2k}\frac{(2k)!}{(s)!(2k-s)!}(-1)^s\times\\&\times\frac{2^{m+l-\frac{1}{m+l+1}-n-s}}{(2k-m-l+\frac{1}{m+l+1}+n)}\oint(-t)^{m-l-1}(1-t)^l(1-\frac{t}{2})^{-m-l-1}\times\\&\times(t)^{s-m-l+\frac{1}{m+l+1}+n}(1-(-1)^{2k-m-l+\frac{1}{m+l+1}+n}(1-t)^{-2k+m+l-\frac{1}{m+l+1}-n})dt.\end{aligned} \tag{93}$$

We find the solution of the sought for integral as follows:

$$\begin{aligned}J=&\frac{\Gamma(1-m+l)\Gamma(m+1)}{\Gamma(1+l)}\frac{1}{2^m}\frac{(l+m)!}{(l-m)!m!}\frac{1}{(m+l+1)}\sum_{k=0}^{\gamma}\frac{\gamma!}{k!(\gamma-k)!}(1)^{\gamma-k}(-1)^k\times\\&\times\sum_{n=0}^{-2k+m+l-1}\frac{(-2k+m+l-1)!}{(n)!(-2k+m+l-1-n)!}(1)^{(-2k+m+l-1-n)}(-1)^n\times\\&\times\sum_{s=0}^{2k}\frac{(2k)!}{(s)!(2k-s)!}(-1)^s\times\\&\times\frac{2^{m+l-\frac{1}{m+l+1}-n-s}}{(2k-m-l+\frac{1}{m+l+1}+n)}(-1)^{-s+m+l-\frac{1}{m+l+1}-n}\times\\&\times(F(s-2l+\frac{1}{m+l+1}+n,m+l+1,s-l+\frac{1}{m+l+1}+n+1,1/2)\frac{\Gamma(l+1)}{\Gamma(1-s+2l-\frac{1}{m+l+1}-n)\Gamma(s-l+\frac{1}{m+l+1}+n+1)}-\\&-(-1)^{2k-m-l+\frac{1}{m+l+1}+n}F(s-2l+\frac{1}{m+l+1}+n,m+l+1,s+1-2k+m,1/2)\frac{\Gamma(1-2k+m+2l-\frac{1}{m+l+1}-n)}{\Gamma(1-s+2l-\frac{1}{m+l+1}-n)\Gamma(s+1-2k+m)}).\end{aligned} \tag{94}$$

REFERENCES

[1] D.V. Khveshchenko, Phys. Rev. Lett. **87**, 246802, (2001).

[2] K. S. Novoselov, A. K. Geim, S. V. Morozov, D. Jiang, Y. Zhang, S. V. Dubonos, I. V. Grigorieva, A. A. Firsov, Science **306**, 666, (2004).

[3] K. S. Novoselov, A. K. Geim, S. V. Morozov, D. Jiang, M. I. Katsnelson, I. V. Grigorieva, S. V. Dubonos, A. A. Firsov, Nature **438**, 197, (2005).

[4] F.T. Vasko, V.V. Mitin, V. Ryzhii, T. Otsuji, Phys. Rev. B **86**, 235424, (2012).

[5] R. Mao, B. D. Kong, C. Gong, S. Xu, T. Jayasekera, K. Cho, and K. W. Kim, Phys. Rev. B **87**, 165410 (2013).

[6] P.R. Wallace, Phys. Rev. **71**, 622, (1947).

[7] D.G.W. Parfitt, M.E. Portnoi, J. Math. Phys. **43**, 4681 (2002), arXiv:math-ph/0205031v1 (2002).

[8] V.A. Fock, Z. Phys. **98**, 145 (1935).

[9] D. Jerome, T.M. Rice, W. Kohn, Phys. Rev. **158**, 462, (1967).

[10] C. H. Sohn, Min-Cheol Lee, H. J. Park, Kyung Joo Noh, H. K. Yoo, S. J. Moon, K. W. Kim, T. F. Qi, G. Cao, Deok-Yong Cho, and T. W. Noh, Phys. Rev. B **90**, 041105(R) (2014).

[11] H. J. Park, C. H. Sohn, D. W. Jeong, G. Cao, K. W. Kim, S. J. Moon, Hosub Jin, Deok-Yong Cho, and T. W. Noh, Phys. Rev. B **89**, 155115 (2014).

[12] T. Stroucken, J.H. Grönqvist, S.W. Koch, Phys. Rev. B **87**, 245428, (2013), arXiv:1305.1780v1 [cond-mat.mes-hall] (2013).

[13] Lyubov E. Lokot, Physica E **68**, 176, (2015), arXiv:1409.0303v1 [cond-mat.mes-hall] (2014).

[14] J. Alicea, M.P.A. Fisher, Phys. Rev. B **74**, 075422, (2006).

[15] V.P. Gusynin, S.G. Sharapov, J.P. Carbotte, Inter. J. Mod. Phys. **21**, 4611, (2007).

[16] T. Stroucken, J.H. Grönqvist, S.W. Koch, Phys. Rev. B **84**, 205445, (2011).

[17] Faris Kadi, Ermin Malic, Phys. Rev. B **89**, 045419, (2014).

[18] Ermin Malic, Torben Winzer, Evgeny Bobkin, Andreas Knorr, Phys. Rev. B **84**, 205406, (2011).

[19] O.V. Gamayun, E.V. Gorbar, V.P. Gusynin, Phys. Rev. B **80**, 165429, (2009).

[20] O.V. Gamayun, E.V. Gorbar, V.P. Gusynin, Ukr. J. Phys. **56**, 688, (2011).

[21] O.L. Berman, R.Ya. Kezerashvili, K. Ziegler, Phys. Rev. A **87**, 042513, (2013), arXiv:1302.4505v1 [cond-mat.mes-hall] (2013).

[22] O.L. Berman, R.Ya. Kezerashvili, K. Ziegler, Phys. Rev. B **85**, 035418 (2012), arXiv:1110.6744v2 [cond-mat.mes-hall] (2011).

[23] R.R. Hartmann, I.A. Shelykh, M.E. Portnoi, Phys. Rev. B **84**, 035437, (2011), arXiv:1012.5517v2 [cond-mat.mes-hall] (2011).

[24] Hongki Min, Rafi Bistritzer, Jung-Jung Su, A.H. MacDonald, Phys. Rev. B **78**, 121401(R), (2008).

[25] Josef Sak, Phys. Rev. B **6**, 3981, (1972).

[26] M. Lindberg and S. W. Koch, Phys. Rev. B. **38**, 3342 (1988).

[27] W.W. Chow, S.W. Koch, and M. Sargent III, *Semiconductor Laser Physics* (Springer, New York, 1994).

[28] W.W. Chow, M. Kira, and S.W. Koch, Phys. Rev. B. **60**, 1947 (1999).

[29] W.W. Chow and M. Kneissl, J. Appl. Phys. **98**, 114502 (2005).

[30] E.M. Lifshitz, L.P. Pitaevski *Statistics Physics, Part II* (Nauka, Moscow, 1978).

[31] A.A. Abrikosov, L.P. Gorkov, I.E. Dzyaloshinski *Methods of Quantum field theory in Statistics Physics* (Moscow, 1962).

[32] H. Haug and S. Schmitt-Rink, Prog. Quant. Electr. **9**, 3 (1984).

[33] B.M. Wul *Excitons in Semiconductors* (Nauka, Moscow, 1971).

[34] L.M. Malard, M.H.D. Guimaraes, D.L. Mafra, M.S.C. Mazzoni, A. Jorio, Phys. Rev. B **79**, 125426, (2009), arXiv:0812.1293v1 [cond-mat.mes-hall] (2008).

[35] V.A. Fock, *Fundamentals of Quantum Mechanics* (Mir, Publishers, Moscow, 1976).

[36] L.D. Landau, E.M. Lifshitz *Quantum Mechanics. Non-Relativistic Theory* (Pergamon, NewYork, 1977).

[37] E.I. Rashba, Sov. Phys. Solid State **2**, 1109 (1960).

[38] R.C. Casella, Phys. Rev. Lett. **5**, 371 (1960).

[39] Y.A. Bychkov, E.I. Rashba, JETP Lett **39**, 78 (1984).

[40] Jiyong Fu, J.Carlos Egues, Phys. Rev. B **91**, 075408 (2015).

[41] S.V. Eremeev, I.A. Nechaev, Yu.M. Koroteev, P.M. Echenique, E.V. Chulkov, Phys. Rev. Lett. **108**, 246802 (2012).

[42] A. Crepaldi, L. Moreschini, G. Autes, C. Tournier-Colletta, S. Moser, N. Virk, H. Berger, Ph. Bugnon, Y.I. Chang, K. Kern, A. Bostwick, E. Rotenberg, O.V. Yazyev, M. Grioni, Phys. Rev. Lett. **109**, 096803 (2012).

[43] A.J. Mildred, S. Dresselhaus, Gene Dresselhaus *Group theory: application to the physics of condensed matter* (Springer-Verlag, Berlin, Heidelberg, 2008).